

## Theory of magnetophonon resonance in quantum wells

V. V. Afonin and V. L. Gurevich

*Wihuri Physical Laboratory, Department of Physics, University of Turku, FIN-20014 Turku, Finland  
and Solid State Physics Division, A. F. Ioffe Institute, 194021 Saint Petersburg, Russia*

R. Laiho

*Wihuri Physical Laboratory, Department of Physics, University of Turku, FIN-20014 Turku, Finland  
(Received 21 March 2000)*

In a polar semiconductor mixed optic phonon-magnetoplasmon vibrations can be trapped within a quantum well. Such localized vibrations effectively interact with the confined electrons of the quantum well. We demonstrate that these excitations can be responsible for the magnetophonon resonance oscillation of the conductivity of quantum wells, i.e., phonon-induced resonant transitions of electrons between the Landau levels. The frequency of the mixed vibrations is shifted, due to the screening effects, towards the frequency of transverse optic vibrations  $\omega_t$ . This can explain the observed shift of the magnetophonon resonance in quantum wells. We give theoretical considerations to determine a (rather narrow) interval of electron concentrations where a two-dimensional magnetophonon resonance is observable.

### I. INTRODUCTION

Magnetophonon resonance (MPR) is the first internal resonance in solids that has been predicted theoretically and subsequently observed experimentally (see the review paper<sup>1</sup>). The resonant condition is met every time when the limiting frequency of an optical phonon equals the cyclotron frequency of an electron,  $\omega_B = eB/mc$ , times some small integer  $\mathcal{N}$ . Since its theoretical prediction<sup>2</sup> and subsequent experimental discovery<sup>3,4</sup> MPR has become a powerful tool to investigate the electron spectra in semiconductors.

First observation of MPR in a quantum well was reported by Tsui *et al.* in their pioneering paper.<sup>5</sup> They observed MPR in a single interface heterojunctions and heterojunction superlattices. Later on the effect was studied by Englert *et al.*,<sup>6</sup> Kido *et al.*<sup>7</sup> and Brummel *et al.*<sup>8</sup>

The purpose of the present paper is to work out a theory of MPR in quantum wells, to provide explanation for the existing experimental data and make predictions for future experiments. We will consider the situation where the well is so narrow that only one electron band of spatial quantization is filled. The magnetic field  $B$  is assumed to be perpendicular to the plane of the well and parallel to  $z$  axis while the external electric field is oriented along  $x$  axis. We will calculate the  $\sigma_{xx}$  component of the conductivity tensor. This is the transport coefficient relating the two-dimensional (2D) current density (averaged over the width of the well) to the applied electric field. The electron states are characterized by the Landau quantum number and by the coordinate of the center of Landau oscillator  $X$ . As is well known<sup>9</sup> in the absence of electron collisions with the impurities and phonons  $\sigma_{xx} = 0$ . This means that one gets a finite expression for  $\sigma_{xx}$  only by taking into account various scattering mechanisms of electrons. We will consider the Frölich<sup>10</sup> interaction between the conduction electrons and polarization optic phonons.

We will show that there is an essential difference between the MPR in 3D and 2D structures. In the 3D case the resonant frequencies  $\omega_{\text{res}}$  are equal to  $\omega_t/\mathcal{N}$ , i.e., are determined by  $\omega_t$ , the frequency of the longitudinal optical phonon. To

the contrary, in the 2D structures the resonance frequencies are expressible with adequate accuracy through  $\omega_t$ , the frequency of the transverse-optic phonon. This agrees with a number of experimental data (for instance, Ref. 8). In the present section we will give some phenomenological considerations concerning the special features of screening of the polarization phonon potential by the 2D electron gas. They enable one to provide explanation as to why the resonant frequency is shifted from  $\omega_t/\mathcal{N}$  to  $\omega_t/\mathcal{N}$ .

As the  $x$  component of the current is proportional to the probability of scattering one can write for it

$$j_x \propto \sum_{nn'} |M_{nn'}|^2 f(\epsilon_n) [1 - f(\epsilon_{n'})] \delta(\epsilon_n - \epsilon_{n'} - \hbar \omega_l). \quad (1.1)$$

Here  $M_{nn'}$  is the matrix element of the electron-optic phonon interaction,  $f(\epsilon_n)$  is the distribution function of the electron with the energy  $\epsilon_n$ . Further on we will neglect the electron degeneracy. In this approximation, the lowest in the electron-phonon interaction, one can expect that the MPR takes place provided the energy difference between a pair of electron levels  $\epsilon_n - \epsilon_{n'} = \mathcal{N}\hbar\omega_B$  coincides with the optic-phonon frequency  $\omega_l$ . Then the current will be proportional to  $\delta(\mathcal{N}\omega_B - \omega_l)$ . This is a system of  $\delta$ -like spikes. Consider now the electron-electron (e-e) interaction, both brought about by an exchange of optic phonons and a direct Coulomb repulsion. We wish to check as to whether the e-e interaction can be treated for 2D systems as a small perturbation. As is well known (Ref. 11, Sec. 43), the variation of transition probability due to a perturbation  $V$  in the second order of the perturbation theory is

$$\delta w = \frac{2\pi}{\hbar} \frac{1}{(\mathcal{N}\omega_B - \omega_{\text{res}})^2} \times \sum_{n,n'} f(\epsilon_n) |V_{nn'} V_{n'n}|^2 \delta(\epsilon_n - \epsilon_{n'} - \hbar \omega_{\text{res}}). \quad (1.2)$$

Near the resonance where  $\omega_{\text{res}} \approx \mathcal{N}\omega_B$  this variation is by no means small. (In 3D case the electron spectrum depends on the  $z$  component of the quasimomentum, which means an extra integration of the denominator over the intermediate states. This, as is shown in Sec. VII, drastically changes the whole situation.)

Let us discuss the role of the screening in propagation of a phonon. To take into account the screening of the Frölich<sup>10</sup> interaction phenomenologically we write the Poisson equation

$$\varepsilon(\omega)\nabla^2\varphi = -4\pi e\delta n, \quad (1.3)$$

where

$$\varepsilon(\omega) = \varepsilon_\infty \frac{\omega_l^2 - \omega^2}{\omega_l^2 - \omega^2}, \quad (1.4)$$

$\varepsilon_\infty$  is the high-frequency dielectric susceptibility,  $\varphi$  is the electrostatic potential,  $\delta n$  is the variation of the electron concentration that is a linear response to the phonon perturbation. Under the resonance conditions this variation should be greatly enhanced. One can represent  $\delta n$  in the following form:

$$\delta n = C \langle 1 | \varphi(z) | 1 \rangle \frac{\psi_1^2(z) \exp(i\mathbf{q}\mathbf{r})}{\mathcal{N}\omega_B - \omega - i\delta}, \quad (1.5)$$

where  $\delta > 0, \delta \rightarrow 0, \psi_1(z)$  is the wave function of transverse quantization of the first band in the quantum well,  $\mathbf{q}$  is the wave vector parallel to the plane of the well,  $C$  is a function of  $\mathbf{q}$ ; its actual form is at the moment of no importance for us.

The denominator in Eq. (1.5) reflects the fact that an electron performing circular motion within the plane of the quantum well perpendicular to  $B$  is perturbed by the optic lattice wave. If the frequency of the wave is a multiple of  $\omega_B$  we have a resonant transition. The transition matrix element due to the factor  $\exp(i\mathbf{q}\mathbf{r})$  does not vanish for *any* integer  $\mathcal{N}$  that is in fact the difference of the Landau quantum numbers of initial and final electron states. This is why multiple magnetophonon resonances are allowed.

The solution of Eq. (1.3) has the form

$$\varphi(z) = \varphi_0 \exp(i\mathbf{q}\mathbf{r}) \int dz' \psi_1^2(z') \exp(-q|z-z'|), \quad (1.6)$$

where  $q = \sqrt{q_x^2 + q_y^2}$ . This is a plane wave localized within the well; the corresponding potential falls off exponentially outside the well<sup>12,13</sup> [see Eq. (4.6)]. The qualitative physical picture does not in fact depend on the value of parameter  $qa$ , where  $a$  is the width of the well. Therefore further on in this section we will discuss the case  $qa \ll 1$ . Then the matrix element on the right-hand side of Eq. (1.5) can be easily calculated and is equal to  $\varphi_0$ .

In order for Eq. (1.6) to be a solution it is necessary that a dispersion relation should be satisfied. Indeed,

$$\nabla^2\varphi = -2q\psi_1^2(z)\varphi_0 \exp(i\mathbf{q}\mathbf{r}).$$

Inserting  $\nabla^2\varphi$  into Eq. (1.3) we get the following dispersion relation:

$$\varepsilon(\omega_{\text{res}}) + \frac{2\pi e^2}{q} \frac{C}{\omega_{\text{res}} - \mathcal{N}\omega_B + i\delta} = 0. \quad (1.7)$$

We are interested in solution of this equation near a resonance where the denominator  $\omega_{\text{res}} - \mathcal{N}\omega_B$  is small. It is only in this region that our approximation (1.5) is valid. Such a solution exists only if  $\omega_l$  is close to  $\mathcal{N}\omega_B$  [see Eq. (1.4)]. Thus the transition takes place due to a dressed vibration having frequency about  $\omega_l$  rather than a bare optic vibration. This means that the resonant peaks are centered near the values  $\mathcal{N}\omega_B = \omega_l$ . The form of the resonance is investigated in detail in Sec. VI (see also Sec. V).

We will show that in the 2D case in polar semiconductors the interaction between the bulk optic phonons and confined electrons leads to a dynamic screening of the optic-phonon potential. As a result, a mixed phonon-plasmon vibration can be localized within a quantum well (Sec. IV). Due to the screening effects such vibration is localized even for the case where one can neglect the difference between the lattice properties within and outside the well. The frequency of the mixed vibrations is shifted towards the frequency of transverse optic vibrations  $\omega_l$ . This can explain the observed shift of the magnetophonon resonance in quantum wells.

As long as the MPR maxima are at the points  $\omega_l/\mathcal{N}$  their widths are determined by the phonon damping (Sec. VIA). The optic-phonon damping is comparatively large even at low temperatures  $k_B T \ll \hbar\omega_{\text{res}}$ . The main process responsible for the damping is the decay of an optic phonon into two acoustic ones (investigated in Appendix A). The damping parameter  $\Gamma$  depends on the anharmonic coefficients. They are sensitive to the perfection of the lattice and, as a rule, it is difficult to make even order-of-magnitude estimates of these.  $\Gamma$ , however, can be in principle measured on experiment, for instance, by Raman scattering of light. Its most probable values range from several K up to several tens of K. Another important point is that  $\Gamma$  within the relevant temperature interval is practically temperature independent.

There can be some competition between the phonon damping  $\Gamma$  and the electron damping  $\Gamma_e$  resulting in a shift of  $\omega_{\text{res}}$ . This competition, however, does not amount to a direct comparison of the two quantities. As soon as the electron damping reaches a critical value  $\Gamma_{ec}$  (Sec. VIB) that, in its turn, depends on the product of the phonon damping and the electron concentration, the MPR maxima begin to shift towards the frequencies slightly lower than  $\omega_l$ . Simultaneously their heights go down. The shift is not too big but can be experimentally discernible. If the electron concentration goes down or the phonon damping goes up the MPR oscillation entirely disappears. In order to see the MPR peak in the frequency region  $\omega_l/\mathcal{N}$  at the values of electron concentration typical for the nanostructures ( $\sim 10^{10} \text{ cm}^{-2}$ ) large values of the damping are necessary and therefore large values of  $\omega_B$ . Very small values of the effective masses are also favorable for such situations. An alternative way to reach resonances at  $\omega_l/\mathcal{N}$  are very small electron concentrations (of the order of  $10^8 \text{ cm}^{-2}$ )—see Eq. (6.3).

All these features are characteristic of a 2D case. As indicated above, in the 3D case the electron spectrum depends on the  $z$  component of the quasimomentum  $k$ . This, as is shown in Sec. VII, changes the whole situation. In the 3D case the screening may play a role in calculation of  $\sigma_{xx}$  only

at comparatively low temperatures where the MPR cannot be observed under the usual conditions.

## II. GENERAL EQUATIONS

To calculate the  $x$  component of the dc current it is convenient to consider the motion of a Landau oscillator as a whole. The conductivity  $\sigma_{xx}$  in the plane of the quantum well is given by (see Ref. 9)

$$\sigma_{xx} = \frac{e^2}{2T} \int_{-\infty}^{\infty} dt \langle \dot{X}(0) \dot{X}(t) \rangle, \quad (2.1)$$

where  $X$  is the operator of coordinate of the center of Landau oscillator in the Heisenberg representation. It commutes with the free-electron Hamiltonian  $\mathcal{H}$  in magnetic field  $B$  as well as with the operator of Coulomb electron-electron interaction. This is a consequence of the quasimomentum conservation in electron-electron collisions. Here  $\langle \dot{X}(0) \dot{X}(t) \rangle$  is the ensemble-averaged correlation function between the velocities of the centers of Landau oscillators. In the present and the following sections we will assume  $\hbar = 1$ ,  $k_B = 1$ , and will restore these symbols only in the resulting formulas.

Now

$$\begin{aligned} \dot{X}(t) &= \sum_{\sigma} \int \psi^{\dagger}(\mathbf{r}, \sigma) i[\mathcal{H}, X] \psi(\mathbf{r}, \sigma) d^3 r \\ &= \sum_{\sigma} \frac{c}{eB} \int \psi^{\dagger}(\mathbf{r}, \sigma) \frac{\partial \hat{U}}{\partial y} \psi(\mathbf{r}, \sigma) d^3 r. \end{aligned} \quad (2.2)$$

Here  $\psi$  is the operator of the electron wave function while  $\hat{U}$  is the operator of phonon field interacting with the electrons. For the time being we consider it as an external random field; later on we will average over all realizations of this field. The expression for  $\sigma_{xx}$  can be presented in such a form (we remind that we calculate the conductivity averaged over the width of the well)

$$\begin{aligned} \sigma_{xx} &= \frac{e^2}{2T} \left( \frac{c}{eB} \right)^2 \int_{-\infty}^{\infty} dt \int \frac{d^2 q}{(2\pi)^2} \int dz \\ &\quad \times \int dz' \frac{q^2}{2} \langle \hat{U}_{-\mathbf{q}}(0, z') \hat{U}_{\mathbf{q}}(t, z) \rangle. \end{aligned} \quad (2.3)$$

We made use of the quasimomentum conservation along the plane of the quantum well. It is convenient to represent  $\hat{U}_{\mathbf{q}}(t, z)$  as [see Eq. (2.2)]

$$\hat{U}_{\mathbf{q}}(t, z) = \hat{n}_{\mathbf{q}}(t, z) U(t, z),$$

where  $\hat{n}_{\mathbf{q}}$  is a Fourier component of the electron-density operator. Equation (2.3) should be averaged over the ensemble, including averaging over the phonon field. It can be performed in two steps. As the first step, we average over the phonon fields in the density matrix by connecting the factors  $\hat{U}_{-\mathbf{q}}(t_1, z')$  and  $\hat{U}_{\mathbf{q}}(t_2, z)$  pairwise. During the second step we average the two phonon fields that are present explicitly in Eq. (2.3). As a result, the correlation function  $\langle \hat{U}_{-\mathbf{q}}(t_1, z') \hat{U}_{\mathbf{q}}(t_2, z) \rangle$  can be presented in the form

$$\begin{aligned} \langle \hat{U}_{-\mathbf{q}}(0, z') \hat{U}_{\mathbf{q}}(t, z) \rangle &= \langle U_{-\mathbf{q}}(0, z') U_{\mathbf{q}}(t, z) \rangle \\ &\quad \times \langle \hat{n}_{-\mathbf{q}}(0, z') \hat{n}_{\mathbf{q}}(t, z) \rangle. \end{aligned} \quad (2.4)$$

Now,

$$\begin{aligned} \langle \hat{n}_{-\mathbf{q}}(0, z') \hat{n}_{\mathbf{q}}(t, z) \rangle &= \sum_{m, l} w_l \exp(-i\omega_{lm}t) \langle m | \hat{n}_{-\mathbf{q}}(0, z') | l \rangle \\ &\quad \times \langle l | \hat{n}_{\mathbf{q}}(0, z) | m \rangle, \end{aligned} \quad (2.5)$$

where  $w_l$  is the probability of occupation of the quantum state  $l$  while  $l, m$  are the exact quantum states of the electron-phonon system as a whole. This correlation function is expressible through exact electron polarization operator, i.e.,

$$\begin{aligned} \langle \hat{n}_{-\mathbf{q}}(z') \hat{n}_{\mathbf{q}}(z) \rangle_{\omega} &= i[\Pi_R(\omega, z', z) \\ &\quad - \Pi_A(\omega, z', z)] \frac{1}{1 - \exp(-\omega/T)}. \end{aligned} \quad (2.6)$$

Here  $\Pi_R(\omega, z', z)$  [ $\Pi_A(\omega, z', z)$ ] is the retarded [advanced] polarization operator that has analytical properties of a boson Green function. Accordingly one has (see Ref. 14, Sec. 36)

$$\begin{aligned} \Pi_R(\omega, z', z) &= \sum_{m, l} w_l \frac{\langle m | \hat{n}(0, z') | l \rangle \langle l | \hat{n}(0, z) | m \rangle}{\omega - \omega_{lm} + i\delta} \\ &\quad \times [1 - \exp(-\omega_{lm}/T)]. \end{aligned} \quad (2.7)$$

As a result,

$$\begin{aligned} \langle \hat{U}_{-\mathbf{q}}(0, z') \hat{U}_{\mathbf{q}}(t, z) \rangle &= \int \frac{d\omega}{2\pi} \langle \hat{n}_{-\mathbf{q}}(z') \hat{n}_{\mathbf{q}}(z) \rangle_{\omega} \\ &\quad \times \langle \hat{U}_{-\mathbf{q}}(-\omega, z') \hat{U}_{\mathbf{q}}(\omega, z) \rangle. \end{aligned} \quad (2.8)$$

One can average over the phonons in the same way. We have

$$\langle \hat{U}_{-\mathbf{q}}(-\omega, z') \hat{U}_{\mathbf{q}}(\omega, z) \rangle = -iN(\omega)[D_R(-\omega) - D_A(-\omega)]. \quad (2.9)$$

Here  $D_R$  ( $D_A$ ) are the exact retarded (advanced) phonon Green functions, and  $N(\omega)$  is the Bose function. We assume that the lattice properties of both components of the heterostructure are practically the same. This means, in particular, that the phonon Green's function in the zeroth approximation should depend on the difference of spatial coordinates.

Inserting Eq. (2.9) into Eq. (2.3) for  $\sigma_{xx}$  we get

$$\begin{aligned} \sigma_{xx} &= \frac{e^2}{4T} \left( \frac{c}{eB} \right)^2 \int_{-\infty}^{\infty} \frac{d\omega}{2\pi} \int \frac{d^2 q}{(2\pi)^2} \\ &\quad \times \int dz \int dz' \frac{q^2 N(\omega)}{1 - \exp(-\omega/T)} \\ &\quad \times [D_R(-\omega) - D_A(-\omega)] [\Pi_R(\omega; z', z) - \Pi_A(\omega; z', z)]. \end{aligned} \quad (2.10)$$

In the lowest approximation of the perturbation theory we have

$$D_{R,A}^{0(q)}(\omega) = |\langle 1 | \hat{U}_{\mathbf{q}} | 0 \rangle|^2 \frac{1}{2} \left( \frac{1}{\omega - \omega_l \pm i\delta} - \frac{1}{\omega + \omega_l \pm i\delta} \right), \quad (2.11)$$

where  $|0\rangle$  and  $|1\rangle$  indicate the states with 0 and 1 optic phonon. For the Frölich interaction<sup>10</sup>

$$|\langle 1 | \hat{U}_{\mathbf{q}} | 0 \rangle|^2 = \frac{4\pi e^2}{q^2 \varepsilon_c}, \quad (2.12)$$

where

$$\frac{1}{\varepsilon_c} = \frac{1}{\varepsilon_\infty} - \frac{1}{\varepsilon_0}.$$

Here  $\varepsilon_0$  and  $\varepsilon_\infty$  are the dielectric susceptibilities for  $\omega \rightarrow 0$  and  $\omega \rightarrow \infty$ , respectively.

Inserting Eq. (2.12) into Eq. (2.10) we get for the 3D space homogeneous case in the lowest approximation in the electron-phonon interaction

$$\begin{aligned} \sigma_{xx} &= \frac{4\pi e^2 c^2 \omega_l}{TB^2 \varepsilon_c} \\ &\times \int \frac{d^2 q dk}{(2\pi)^3} \frac{q^2}{q^2 + k^2} \frac{N(\omega_l)}{1 - \exp(-\omega_l/T)} \\ &\times \text{Im} \Pi_A(\omega_l, \mathbf{q}, k). \end{aligned} \quad (2.13)$$

This equation was obtained by Gurevich and Firsov in Ref. 2.

### III. NAÏVE PERTURBATION APPROACH IN 2D CASE

To begin with, we will consider a well where the electrons are confined by a parabolic potential

$$U(z) = \frac{m}{2} \omega_0^2 z^2. \quad (3.1)$$

It will be seen that such an assumption facilitates the calculations without seriously affecting the result in the general case. We assume that the interlevel distance between the oscillator levels satisfies the condition  $\hbar \omega_0 \gg T$ , so that only the 2D band associated with the lowest vibrational level is occupied.

Our problem is spatially inhomogeneous along the  $z$  direction. Accordingly, we introduce the coordinates

$$\Delta z = z_1 - z_2, \quad Z = (z_1 + z_2)/2. \quad (3.2)$$

The corresponding  $z$  components of the quasimomentum we will denote by  $k$  and  $K$ . Then

$$\Pi_R(\omega, \mathbf{q}, z_1, z_2) = \psi_1(z_1) \psi_1(z_2) \Pi_R^{(2)}(\omega, \mathbf{q}), \quad (3.3)$$

where  $\Pi_R^{(2)}(\omega, \mathbf{q})$  is the 2D polarization operator calculated by Gurevich and Shtengel<sup>13</sup> (see also Sondheimer and Wilson<sup>15</sup>) that is given by

$$\begin{aligned} \Pi_R^{(2)}(\omega, \mathbf{q}) &= -2n_s \exp \left[ -\frac{1}{2} (qa_B)^2 \coth \alpha \right] \\ &\times \sum_{\mathcal{N}=-\infty}^{\infty} \frac{\sinh \mathcal{N} \alpha}{\omega - \mathcal{N} \omega_B + i\delta} I_{\mathcal{N}} \left( \frac{q^2 a_B^2}{2 \sinh \alpha} \right). \end{aligned} \quad (3.4)$$

Here  $a_B^2 = c\hbar/eB$ ,  $n_s$  is the 2D electron concentration

$$\begin{aligned} n_s &= \frac{1}{\pi} a_B^{-2} \frac{\cosh(\hbar \Omega_0/2k_B T)}{\sinh(\hbar \omega_B/2k_B T)} \\ &\times \exp \left( \frac{\mu}{k_B T} - \frac{\hbar \omega_0}{2k_B T} \right); \quad \alpha = \frac{\hbar \omega_B}{2k_B T}. \end{aligned} \quad (3.5)$$

$\hbar \Omega_0$  is the difference between the two electron spin level positions. We wish to emphasize that  $\Pi_R^{(2)}(\omega, \mathbf{q})$  is a purely 2D polarization operator depending neither on  $k$  nor on  $K$ . For a well of parabolic form we have

$$\Pi_R(\omega, \mathbf{q}) = \exp(-\mathcal{A}/2) \Pi_R^{(2)}(\omega, \mathbf{q}), \quad (3.6)$$

where

$$\mathcal{A} = k^2 l^2 + \frac{1}{4} K^2 l^2 \quad (3.7)$$

(here  $l = 1/\sqrt{m\omega_0}$  is the amplitude of the zero-point vibrations).

Now we embark on calculation of  $\sigma_{xx}$  for a quantum well. As in the zeroth approximation in the electron-phonon interaction the phonon Green's function is spatially homogeneous and the polarization operator at  $K=0$  enters the equation for  $\sigma_{xx}$ . However, as the  $z$  component of the electron's quasimomentum is not conserved one should integrate over all the  $k$ . As a result, the electron-phonon interaction is

$$V^{(2)}(\mathbf{q}) = \frac{4\pi e^2 \omega_l}{\varepsilon_c} \int_{-\infty}^{\infty} \frac{dk}{2\pi} \frac{\exp(-k^2 l^2/2)}{k^2 + q^2}. \quad (3.8)$$

One can easily see that if the characteristic values of  $k^2 l^2$  are much smaller than 1 the exponent in the integrand can be replaced by 1 and one gets the standard expression for the 2D electron-phonon interaction

$$V^{(2)} = \frac{2\pi e^2 \omega_l}{\varepsilon_c q}. \quad (3.9)$$

Physically this case means a weak variation of the effective electron-phonon interaction over the width of the well. Taking into consideration the asymptotic behavior of  $I_{\mathcal{N}}$  as well as the exponential factor in Eq. (3.4) the inequality  $q^2 a_B^2 \ll 1$  can be rewritten as

$$l \ll \frac{\sinh(\omega_B/4T)}{\sqrt{\sinh(\omega_B/2T)}} a_B. \quad (3.10)$$

For arbitrary relations between  $l$  and  $a_B$ :

$$V^{(2)}(q^2) = \frac{2\pi e^2 \omega_l}{\varepsilon_c q} \exp(q^2 l^2/2) [1 - \Phi(q l/\sqrt{2})], \quad (3.11)$$

where  $\Phi(x)$  is the error function:

$$\Phi(x) = \frac{2}{\sqrt{\pi}} \int_0^x dt \exp(-t^2).$$

Our purpose is to investigate the magnetophonon resonance. This means that we are interested in the situation where the integral over  $\omega$  in Eq. (2.10) is dominated by the frequencies satisfying the inequality

$$|\mathcal{N}\omega_B - \omega| \ll \omega_B. \quad (3.12)$$

Then one can retain in Eq. (3.4) a single term with  $\mathcal{N} \approx \omega/\omega_B$  while  $\text{Im} \Pi_R(\omega_l)$  is proportional to  $\delta(\mathcal{N}\omega_B - \omega_l)$  and we have

$$\sigma_{xx} = \frac{2\pi n_s c^2 \hbar^2}{k_B T B^2} \sinh \frac{\mathcal{N}\omega_B}{2k_B T} \delta(\mathcal{N}\omega_B - \omega_l) \mathcal{J}_N(\omega_B), \quad (3.13)$$

$$\begin{aligned} \mathcal{J}_N(\omega) &= \int \frac{d^2q}{(2\pi)^2} q^2 I_N \left( \frac{a_B^2 q^2}{\hbar \omega} \right) \\ &\times \exp \left[ -\frac{a_B^2 q^2}{2} \coth \left( \frac{\hbar \omega_B}{2k_B T} \right) \right] V^{(2)}(q^2). \end{aligned} \quad (3.14)$$

Equation (3.13) exhibits a number of  $\delta$ -like resonant spikes. Such sharp spikes originate in the fact that in the one-band approximation of 2D situation the only type of electron motion is their quantized motion in the magnetic field. A comparison with the 3D case shows that instead of  $\delta(\mathcal{N}\omega_B - \omega_l)$  there appears a resonant factor

$$\frac{1}{\sqrt{\pi} q_B v_T} \exp \left[ -\frac{(\mathcal{N}\omega_B - \omega_l)^2}{(q_B v_T)^2} \right], \quad (3.15)$$

where  $q_B$  is the component of the wave vector parallel to  $B$ . A logarithmic form of the resonant peak in  $\sigma_{xx}$  is due to the electron motion along the magnetic field.

When inequality (3.10) is satisfied one can easily give an estimate of integral  $\mathcal{J}_N$ . We have

$$\begin{aligned} \mathcal{J}_N(\omega) &= \frac{\sqrt{2} e^2 \omega_l}{\varepsilon_c a_B^3} \left( \sinh \frac{\omega}{2k_B T} \right)^{3/2} \int_0^\infty dx \sqrt{x} I_N(x) \\ &\times \exp \left( -x \sinh \frac{\omega}{2k_B T} \coth \frac{\omega_B}{2k_B T} \right). \end{aligned} \quad (3.16)$$

Below we will see (Sec. VI) that in fact Eq. (3.13) is never valid in the 2D case under the assumptions it has been derived. One feels that in fact the collisional broadening should always play a role. We will not discuss the broadening of the MPR peaks in this case as the problem has been investigated in detail in Ref. 16. We will see, however, that the width of the Landau levels necessary to get the result (3.13) may reach several hundred K for  $n_s$  slightly exceeding  $10^{10} \text{ cm}^{-2}$ .

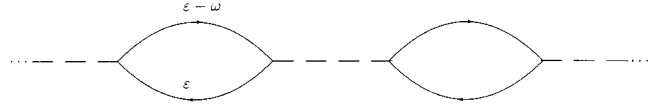


FIG. 1. A chain of electron loops connected by the phonon lines.

#### IV. BARE ELECTRON-PHONON INTERACTION

In this section we will show how to take into consideration the screening in a quantum well where one 2D band is occupied. This will result in a shift of the magnetophonon resonant frequencies from  $\omega_l$  towards  $\omega_r$ . We will take into consideration the Fröhlich electron-phonon interaction screened by the conduction electrons of the quantum well. Following Ref. 17, one should add to the phonon propagator  $D^{(0)}$  the Coulomb electron-electron interaction  $4\pi e^2/(q^2 + k^2)\varepsilon_\infty$ . Then the full propagator in the zeroth approximation is

$$\mathcal{F} = D^{(0)} + \frac{4\pi e^2}{(q^2 + k^2)\varepsilon_\infty} = \frac{4\pi e^2}{q^2 \varepsilon(\omega)}, \quad \varepsilon(\omega) = \varepsilon_\infty \frac{\omega_l^2 - \omega^2}{\omega_l^2 - \omega^2}. \quad (4.1)$$

We remind that  $\omega_r^2 = \omega_l^2(1 - \varepsilon_\infty/\varepsilon_c)$ .

Now we should surmise as to how to treat a spatially inhomogeneous situation with a quantum well. Assuming that the gas approximation is valid, it is sufficient to sum up the loop diagrams depicted in Fig. 1. To avoid excessive proliferation of notation we will indicate here only the  $k$  dependence, i.e., the dependence on the  $z$  component of the electron quasimomentum.

Introducing Fourier components regarding the sum and difference variables introduced in Eq. (3.2) one comes to the conclusion that the diagram in Fig. 1 corresponds to the following analytical expression:

$$\begin{aligned} &\int dk_1 dk_2 dk_3, \dots, \mathcal{F}(k_1) \Pi \left( \frac{k_1 + k_2}{2}, k_1 - k_2 \right) \\ &\times \mathcal{F}(k_2) \Pi \left( \frac{k_2 + k_3}{2}, k_2 - k_3 \right) \mathcal{F}(k_3) \dots \end{aligned} \quad (4.2)$$

Here the first argument of  $\Pi$  is the Fourier component of the difference of coordinates while the second argument is the Fourier component of the sum of coordinates. It follows from Eqs. (3.6), (3.7), and (4.2) a factorization of the dependence on quasimomenta. In other words, we get a geometric progression with the index  $\Pi^{(2)}(q, \omega) V^{(f)}(q, \omega)$  where

$$V_{R,A}^{(f)}(q, \omega) = \frac{4\pi e^2}{\varepsilon_{R,A}(\omega)} \int_{-\infty}^\infty \frac{dk}{2\pi} \frac{\exp(-k^2 l^2/2)}{k^2 + q^2}. \quad (4.3)$$

This means that to calculate  $\sigma_{xx}$  for a quantum well where only the lowest 2D band is occupied it is sufficient to solve the problem where 2D electrons interact with each other via the potential  $V^{(f)}$ .

We emphasize that the potential  $V^{(f)}(q, \omega)$  is practically independent of the form of the well. If the condition (3.10) is satisfied,  $V^{(f)}(q, \omega)$  does not depend on the form of the well at all. However the difference remains small even for  $kl \sim 1$ . One can see it from Ref. 13 for a well with infinitely high rectangular walls. Indeed, for the model adopted in Ref.

13, using phenomenological considerations, the following equation for  $V^{(f)}(q, \omega)$  was obtained:

$$V^{(f)}(q, \omega) = \frac{2\pi e^2}{q\varepsilon(\omega)} f(qa), \quad (4.4)$$

where

$$\varphi = \phi_0 \exp[i(\mathbf{q}\mathbf{r} - \omega t)] \times \begin{cases} \exp(qa/2) \{ [1 + (a^2 q^2 / 2\pi) \cos^2(\pi z/a)] - \cosh(qz) \}, & |z| \leq a/2 \\ \sinh(qa/2) \exp[q(a/2 - |z|)], & |z| \geq a/2 \end{cases} \quad (4.6)$$

The exact formulas for  $f(q)$  should depend on the form of the confining potential through the wave function  $\psi_1(z)$ . However, the difference between various confining potentials is in general not too big and the asymptotic behavior is the same

$$f(q) = \begin{cases} 1, & qa \ll 1 \\ 2/qa, & qa \gg 1. \end{cases} \quad (4.7)$$

In fact such heterostructures as GaAs-Ga<sub>x</sub>Al<sub>1-x</sub>As can exhibit a two-mode behavior, i.e., existence of pairs of two different  $\omega_l$  and  $\omega_r$  optic frequencies in the materials making the heterostructure (such as GaAs and GaAlAs). The reflectivity experiments (for instance, Ref. 18) show behavior of such a sort. This fact, however, should not change the physical situation in regard to the localization. Indeed, the localization of an optic phonon within the quantum well because of the screening can be only enhanced due to the existence of the interfaces.

## V. MPR IN QUANTUM WELLS

According to Eq. (2.10) the conductivity  $\sigma_{xx}$  is expressed through the phonon Green's function with regard to screening. This means that we should sum up all the electron loops (see Fig. 1) connected by the effective interaction lines. Each such line  $V^{(f)}$  can be represented as a sum of the phonon propagator and the Coulomb interaction integrated over  $k$  as is indicated in Sec. IV and expressed by Eq. (4.3).

One should, however, observe the following important point. Both ends of a chain *should be ordinary phonon lines*  $D^{(0)}$  *without Coulomb interaction*. This is due to the fact (mentioned in Sec. II) that the operator  $X$  commutes with the electron-electron interaction operator [see Eq. (2.2)] as the latter conserves the electron quasimomentum.

Let us introduce two quantities that we will need below. These are the bare Coulomb interaction

$$V_0(\mathbf{q}) = \frac{4\pi e^2}{\varepsilon_\infty} \int_{-\infty}^{\infty} \frac{dk}{2\pi} \frac{\exp(-k^2 l^2/2)}{k^2 + q^2} \quad (5.1)$$

$$f(q) = (4/a^2) \int_{-a/2}^{a/2} dz \int_{-a/2}^{a/2} dz' \cos^2(\pi z/a) \cos^2(\pi z'/a) \times \exp(-q|z - z'|). \quad (4.5)$$

Here  $\psi_1(z) = \sqrt{2/a} \cos(\pi z/a)$  entering this and the following equation is the wave function of transverse quantization corresponding to the lowest level. The space and time dependence of electrostatic potential accompanying the localized phonon propagation is

and the zero-order phonon propagator (without regard of Coulomb interaction, except for the electron-phonon vertices  $\sqrt{V^{(2)}}(\mathbf{q})$  that it is convenient to include into a zero-order phonon line)

$$D_{R,A}^{(0)}(\omega) = \frac{1}{2} V^{(2)}(q) \left( \frac{1}{\omega - \omega_l \pm i\delta} - \frac{1}{\omega + \omega_l \pm i\delta} \right). \quad (5.2)$$

If one had the full interaction in all the vertices one would have had as a result of summation of the progression the following equation for the full propagator  $D^{(f)}$ :

$$D_{R,A}^{(f)} = \frac{V_{R,A}^{(f)}}{1 + V_{R,A}^{(f)} \Pi_{R,A}^{(2)}}. \quad (5.3)$$

The outer lines, however, should represent only the phonon propagators. It is convenient to add to the outer lines the bare Coulomb interactions  $V_0(q)$  to get the full lines  $D^{(f)}$  and then to subtract the same interactions. As a result, one gets instead of Eq. (5.3):

$$D_{R,A}^{(f)} - V_0 + \frac{2V_0 V^{(f)}}{\Pi^{-1} + V^{(f)}} = \Delta \mathcal{D}, \quad (5.4)$$

where

$$\Delta \mathcal{D} = \frac{V_0^2}{\Pi^{-1} + V^{(f)}}. \quad (5.5)$$

We will show that MPR is determined by the last term in Eq. (5.4). In the approximation where Eq. (3.12) is satisfied, the difference  $\Pi_R - \Pi_A$  is proportional to the  $\delta$  function so that one gets

$$\sigma_{xx} = -\frac{ic^2}{TB^2} \int \frac{d^2 q}{(2\pi)^2} q^2 \frac{N(\mathcal{N}\omega_B)}{1 - \exp(-\mathcal{N}\omega_B/T)} \times \mathcal{R}_{\mathcal{N}}[\Delta \mathcal{D}_R(\mathcal{N}\omega_B) - \Delta \mathcal{D}_A(\mathcal{N}\omega_B)], \quad (5.6)$$

where

$$\mathcal{R}_{\mathcal{N}} = 2n_s \exp\left[-\frac{1}{2} q^2 (a_B)^2 \coth \alpha\right] \sinh(\mathcal{N}\alpha) I_{\mathcal{N}}\left(\frac{q^2 a_B^2}{2 \sinh \alpha}\right) \quad (5.7)$$

is the negative residue of  $\Pi^{(2)}$  [Eq. (3.5)] while  $\mathcal{N}$  is the number of the MPR peak. Finally

$$\sigma_{xx} = \frac{2\pi\varepsilon_c n_s c^2 \hbar^2}{\varepsilon_\infty \omega_l k_B T B^2} \sinh \frac{\hbar \omega_l}{2k_B T} \mathcal{J}_{\mathcal{N}}(\omega_l) \delta[\varepsilon^{-1}(\mathcal{N}\omega_B)] \quad (5.8)$$

or

$$\sigma_{xx} = \frac{\pi\varepsilon_c n_s c^2 \hbar^2 (\omega_l^2 - \omega_t^2)}{\varepsilon_\infty \omega_l \omega_l k_B T B^2} \sinh \frac{\hbar \omega_l}{2k_B T} \delta(\mathcal{N}\omega_B - \omega_l) \mathcal{J}_{\mathcal{N}}(\omega_B), \quad (5.9)$$

where  $\mathcal{J}_{\mathcal{N}}(\omega)$  is given by Eq. (3.14). Thus instead of the resonance condition (3.13) determined by the frequency  $\omega_l$  one has the condition (5.9) where  $\omega_l$  is replaced by  $\omega_t$ .

The contributions of all the rest terms in Eq. (5.4) are formally proportional to the expressions of the type  $\varepsilon\delta(\varepsilon)$ . Therefore they vanish in this approximation.

## VI. FINITE WIDTH OF MPR LINE

### A. Phonon damping $\Gamma$

We will start with taking into account the phonon damping. Finite optic-phonon damping is due to the decay of an optic phonon into two acoustic ones (see Appendix A). Technically it can be taken into account by replacement  $\omega \rightarrow \omega \pm i\Gamma$  in the retarded and advanced phonon Green functions, respectively, where  $\Gamma$  is the damping parameter. One can easily see that in such a case the MPR acquires a finite width that results in the following replacement in Eq. (5.8)

$$\delta(\varepsilon^{-1}) \rightarrow \frac{1}{\pi} \text{Im} \varepsilon_R. \quad (6.1)$$

Here

$$\frac{1}{\pi} \text{Im} \varepsilon_R = \frac{\omega_l^2 - \omega_t^2}{2\pi\omega_l} \frac{\Gamma}{(\mathcal{N}\omega_B - \sqrt{\omega_l^2 + \Gamma^2})^2 + \Gamma^2}. \quad (6.2)$$

This result is valid provided that

$$\Gamma^2 \ll \omega_B^2. \quad (6.3)$$

We see that according to Eq. (6.3) both the shift of the resonant maximum and its width are determined by the parameter  $\Gamma$ . In Appendix B we will show, however, that the shift of the resonance frequency is in fact determined by the

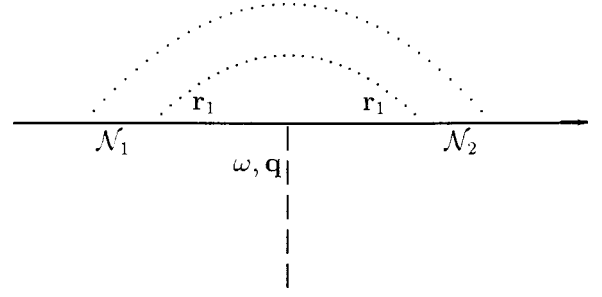


FIG. 2. Electron-phonon vertex with impurity line corrections (dotted lines).

phonon dispersion rather than the damping parameter  $\Gamma$ . In a real situation, however, one can neglect all these shifts. At the same time, the damping parameter determines the width of the resonance.

### B. Electron damping $\Gamma_e$

Now we turn to consideration of the electron damping  $\Gamma_e$ . We will assume that the main mechanism of electron relaxation is a short-range impurity scattering and validity of the following inequality:

$$\Gamma_e \ll \omega_B. \quad (6.4)$$

As is shown by Laikhtman and Altshuler<sup>19</sup> (see also Ref. 20) the self-energy diagram is a periodic function of energy with the period  $\omega_B$  and has the following form:

$$\Sigma_{\mathcal{N}}(E) = \frac{1}{2} [E - \mathcal{N}\omega_B \pm i\sqrt{4\Gamma_e^2 - (E - \mathcal{N}\omega_B)^2}] \quad (6.5)$$

provided that  $|E - \mathcal{N}\omega_B| \ll \Gamma_e$ . In this case the electron Green's function has a non-Lorentzian form with the characteristic width  $\Gamma_e$  given by (see Ando and Uemura)<sup>21,22</sup>

$$\Gamma_e^2 = \omega_B^2 / 2\pi\tau, \quad (6.6)$$

where  $\tau$  is the relaxation time for  $B=0$  obtained by assuming the same scatterers.

Let us discuss the corrections to the vertex depicted in Fig. 2. The renormalization of the vertex would be important if the index of the geometric progression were close to 1. This would be the case for the resonant values of  $\omega \sim \mathcal{N}\omega_B$  had one been able to neglect the dependence on the phonon wave vector  $\mathbf{q}$ . Later, of all the analytic expressions of the diagram in Fig. 2, we will write only the relevant factors. They are

$$\sum_{\mathcal{N}_1 \mathcal{N}_2} \int d^2 r_1 \frac{\psi_{\mathcal{N}_1}(\mathbf{r}_1) \exp(i\mathbf{q}\mathbf{r}_1) \psi_{\mathcal{N}_2}(\mathbf{r}_1)}{[E - \mathcal{N}_1 \omega_B - \Sigma_{\mathcal{N}_1}(E)] [E + \omega - \mathcal{N}_2 \omega_B - \Sigma_{\mathcal{N}_2}^*(E + \omega)]},$$

where an asterisk denotes a complex conjugation.

Because of the orthogonality of the wave functions with different quantum numbers  $\mathcal{N}$  the index of the geometric progression tends to zero as a power of  $(qa_B)^2$  when  $q \rightarrow 0$ . It goes down provided that  $(qa_B)^2$  is big enough as well. As the MPR is dominated by  $(qa_B)^2 \sim \mathcal{N}$  it is clear that

the renormalization of the vertex, if relevant at all, brings a factor of the order of unity. For the order-of-magnitude estimates it will be sufficient to use the Lorentzian form of  $\Pi^{(2)}(\omega, \mathbf{q})$ . Moreover, in the resonance approximation one should retain only the resonant term of all the series for  $\Pi_R^{(2)}(\omega, \mathbf{q})$

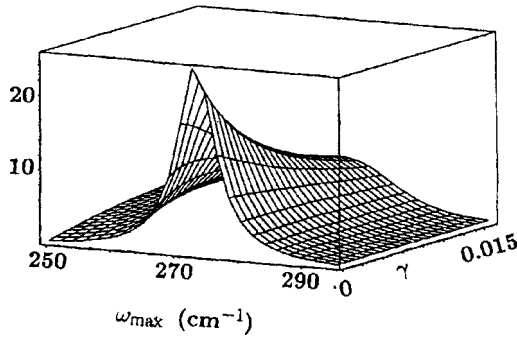


FIG. 3. 3D plot of the form and position of MPR maximum for  $\mathcal{N}=3$  [Eq. (6.8)].

$$\Pi_R^{(2)}(\omega, \mathbf{q}) = -\frac{\mathcal{R}_\mathcal{N}(\omega, \mathbf{q})}{\omega - \mathcal{N}\omega_B + i\Gamma_e}. \quad (6.7)$$

One can calculate the integral over frequency in Eq. (5.9) for  $\sigma_{xx}$  taking the residues in the poles  $\omega = \mathcal{N}\omega_B \pm i\Gamma_e$ . This results in replacement of  $\delta(\varepsilon^{-1})$  by

$$\Delta \equiv \frac{1}{\pi} \frac{\text{Im} \varepsilon_A^{-1} + 2\gamma}{(2\gamma + \text{Im} \varepsilon_A^{-1})^2 + (\text{Re} \varepsilon_A^{-1})^2}, \quad (6.8)$$

where

$$\gamma = \frac{\Gamma_e}{\bar{\omega}}; \quad \bar{\omega} = \frac{2\pi e^2}{q} \mathcal{R}_\mathcal{N}(\mathcal{N}\omega_B, \mathbf{q}).$$

For small values of  $\gamma$ , Eq. (6.8) turns into  $\text{Im} \varepsilon_R(\omega_l)$  and one can neglect the term  $2\gamma$  in the numerator of Eq. (6.8). When, however,  $\text{Im} \varepsilon_A^{-1}/2\gamma \ll 1$ , Eq. (6.8) has a large field-independent term, which is usually omitted during analysis of the experimental data. Therefore in our numerical calculations, to get an idea about the position of the MPR maximum, we computed the derivative of Eq. (6.8) over  $\omega = \mathcal{N}\omega_B$ .

It follows from Eq. (6.8) that after  $\gamma$  has reached the critical value  $(1/2)|\varepsilon_A^{-1}(\omega_l)|$  the amplitude of the peak goes down while its position slightly moves—see Figs. 3 and 4. It means that the shift of the resonance begins provided that  $\Gamma_e$  exceeds the characteristic value  $\Gamma_{ec}$  given by

$$\Gamma_{ec} = \frac{2\pi e^2 a_B n_s}{\hbar \varepsilon_\infty} \frac{\Gamma}{\omega_l - \omega_t}. \quad (6.9)$$

For  $n_s \sim 6 \times 10^{10}$ ,  $\mathcal{N}=3$  and  $\Gamma \sim 5$  K this gives  $\Gamma_{ec} \sim 10$  K.

This estimate can be reformulated in a different way, as the electron concentration goes down, the MPR peak should also go down. This imposes the following condition on the electron concentration where such a decrease of the resonant peak begins:

$$n_s \lesssim n_{\text{down}} \equiv \frac{\varepsilon_\infty \hbar (\omega_l - \omega_t)}{2\pi e^2 a_B} \frac{\Gamma_e}{\Gamma}.$$

For GaAs  $n_{\text{down}} \approx 2 \times 10^{10} \text{ cm}^{-2} (\Gamma_e/\Gamma)$ . One can visualize the physical meaning of the concentration  $n_{\text{down}}$  in the following way. For low electron concentrations the screening becomes inefficient. As a result, the MPR maximum we have discussed goes down (see below) and the phonon itself can

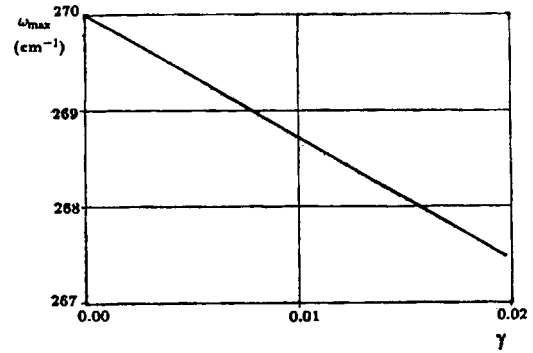


FIG. 4. Shift of the MPR maxima's positions.

become delocalized (provided one entirely neglects a possible role of the interfaces). We emphasize that the efficiency of screening is in fact determined by the ratio  $n_s \Gamma/\Gamma_e$ . At even lower concentrations the MPR oscillation disappears.

As can be seen from numerical calculation (see Figs. 4 and 5) when the electron concentration  $n_s$  diminishes so that it becomes of the order of  $n_{\text{down}}$ , the peak amplitudes at first go down relatively rapidly. Then the resonances become much less sharp and at the same time their positions are shifted towards low frequencies. The typical shift is about 10% of the peak's width—see Fig. 5. Such behavior of the resonant maximum is related to the fact that on the one hand the resonance is due to the zero of  $\varepsilon^{-1}$  at  $\omega_l = \mathcal{N}\omega_B$  while on the other hand  $\varepsilon^{-1}$  has a maximum at  $\omega_t$ , i.e., relatively far away from  $\omega_l$  as compared to  $\Gamma$  and  $\Gamma_e$ . One should keep in mind that as soon as  $\text{Im}(\varepsilon_A^{-1}/2\gamma)$  reaches a value of the order of 1, a contribution of the denominator of Eq. (6.8) that has the opposite sign becomes important and the principal field-independent term is partially cancelled. As a result, the MPR maximum is shifted not towards higher frequencies [as one could have judged by the numerator of Eq. (6.8)] but in the opposite direction (Fig. 4).

We would like to draw attention to the following point. Brummel *et al.* in Ref. 8 discussing a possible role of screening in 2D MPR, discarded this possibility for the reason it would be strongly temperature dependent. However [see Eqs. (6.8) and (6.9)] the positions and forms of the resonance maxima are determined by the attenuation parameters that depend on temperature but weakly in the relevant temperature interval.

In addition to the aforementioned limitation on the electron concentration from below, there is also a limitation from

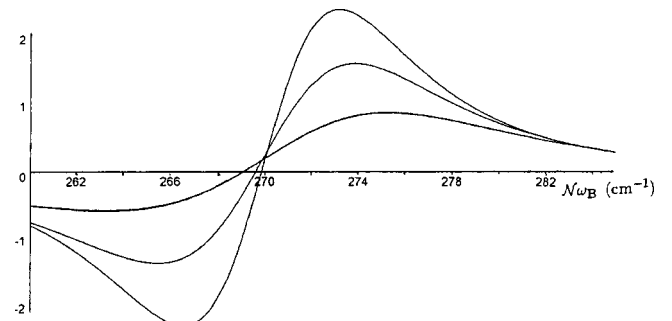


FIG. 5. Derivative  $\partial\Delta/\partial(\mathcal{N}\omega_B)$  [see Eq. (6.8)] for  $\gamma=0.001$ ;  $\gamma=0.003$ ; and  $\gamma=0.007$  (from the upper curve downward) at  $\omega_l = 270 \text{ cm}^{-1}$ ,  $\omega_t = 300 \text{ cm}^{-1}$ , and  $\gamma = 5 \text{ cm}^{-1}$ .



above. To investigate it we calculate, as above, the integral over frequencies in Eq. (5.9) for  $\sigma_{xx}$  by taking the residues at the poles

$$\omega = \mathcal{N}\omega_B + (2\pi e^2/q)\mathcal{R}_N(q)\varepsilon_A^{-1}(\omega).$$

For simplicity, we have discarded here  $\Gamma_e$ . This equation can be solved by iterations. In the lowest approximation  $\omega = \mathcal{N}\omega_B$ . The next iteration is the second term at  $\omega = \mathcal{N}\omega_B$ . Now, of all the series (3.4) for  $\Pi^{(2)}$ , we keep only the single resonant term. This can be justified if the imaginary part of the root we have obtained is smaller than  $\omega_B$ . This requirement can be formulated as

$$n_s \lesssim n_{\text{up}} \equiv \frac{\varepsilon_{\infty} \hbar (\omega_l - \omega_t)}{2\pi e^2 a_B} \frac{\omega_B}{\Gamma}. \quad (6.10)$$

For the values of parameters accepted above, the concentration on the right-hand side of Eq. (6.10) is

$$n_s \approx 5 \times 10^{11} \text{ cm}^{-2}.$$

One can offer a simple physical interpretation for this limitation. The MPR peaks are associated with transitions between one-electron levels. Naturally the e-e interaction that does not conserve the one-electron energy results in a broadening of the one-electron levels. When the broadening becomes of the order of interlevel distance, the MPR peaks disappear. The oncoming degeneracy can enhance this process. Qualitatively such a concentrational dependence *with a maximum at some intermediate concentration* provides a theoretical interpretation of the results of Ref. 23.

It is interesting to know as to whether under any circumstances the MPR oscillation exists for  $\omega_l = \mathcal{N}\omega_B$ . Let us analyze for this purpose the evolution of the MPR when  $\Gamma_e$  goes up. The term we were discussing above tends to zero. In the region of magnetic fields  $\omega_B = \omega_l/\mathcal{N}$  it is replaced by another resonant term emerging from  $D^{(f)}$  [Eq. (5.4)]. Inserting expression for  $D^{(f)}$  into the equation for  $\sigma_{xx}$  [Eq. (5.6)] and using the identity

$$\frac{\omega_l - \omega_t}{\varepsilon_{\infty}} = \frac{\omega_l}{2\varepsilon_c},$$

we get after some algebra Eq. (3.13) with the replacement

$$\delta(\mathcal{N}\omega_B - \omega_l) \rightarrow \frac{1}{\pi} \frac{\Gamma}{(\mathcal{N}\omega_B - \sqrt{\omega_l^2 + \Gamma^2})^2 + \Gamma^2}. \quad (6.11)$$

This result is valid provided that

$$\Gamma_e \gg \frac{2\pi e^2 (\omega_l - \omega_t)}{q_c \varepsilon_{\infty} \Gamma} \mathcal{R}(q_c), \quad (6.12)$$

where  $q_c$  is the characteristic value of  $q$ .

Mathematically this inequality is needed to suppress the loop diagrams that would be proportional to  $1/(\omega - \mathcal{N}\omega_B + i\delta)$  (without regard of  $\Gamma_e$ ). This demands a large electron damping. (It is interesting to note that this statement can be related not only to MPR but to a number of other phenomena in 2D situation as one is allowed to ignore the electron loops when the damping is large.) The inequality (6.12) ensures the suppression. In this case one can neglect the screening of the

Frölich interaction by the free carriers. This is why the 2D case is much less favorable for observation of MPR at  $\mathcal{N}\omega_B = \omega_l$  than the 3D case (see Sec. VII). For  $q_c \sim 1/a_B$ , Eq. (6.12) can be written as

$$\Gamma_e \gg \frac{4\pi e^2 a_B \omega_l n_s}{\Gamma \varepsilon_c k_B}. \quad (6.13)$$

This result is given in K. For  $n_s = 4 \times 10^{10}$  we get as an order-of-magnitude estimate of several hundred K, whereas  $\hbar\omega_B$  for  $\mathcal{N}=3$  is about 130 K. One can hardly expect the MPR oscillation under these conditions. Indeed, in order to observe a MPR peak in this frequency region at the electron concentration typical for the nanostructures ( $\sim 10^{10} \text{ cm}^{-2}$ ) big values of the dampings are needed as well as large values of  $\omega_B$ . As has been indicated above, very small values of the effective masses are favorable for such a situation. An alternative way to reach the MPR resonances at  $\omega_l/\mathcal{N}$  are small electron concentrations.

## VII. COMPARISON OF 2D AND 3D CASES

In the present section we are discussing the following important point. Why in the 3D case, where there is a free-electron motion along the  $B$ -direction, does MPR not shift towards  $\omega_l/\mathcal{N}$ ? The shift exists provided that

$$\frac{4\pi e^2}{\varepsilon(\omega) q_c^2} \Pi^{(3)}(\omega, q_c) \Big|_{\omega=\omega_l} \geq 1, \quad (7.1)$$

$q_c$  being of the order of  $1/a_B$ .

The principal difference between the 2D and 3D cases is in the singularity of 2D polarization operator existing provided one neglects the electron damping. In the 3D case the polarization operator  $\Pi^{(3)}$ , because of dependence of the electron energy on the projection of electron quasimomentum on the magnetic field  $q_B$ , has a finite amplitude and width. For what follows it is sufficient to know its imaginary part<sup>2</sup>

$$\begin{aligned} \text{Im } \Pi_R^{(3)}(\omega, \mathbf{q}, q_B) &= \frac{\sqrt{\pi} n}{|q_B| v_T} \exp\left[-\frac{1}{2}(q a_B)^2 \coth \alpha\right] \\ &\times \sum_{N=-\infty}^{\infty} \exp\left[-\frac{(\mathcal{N}\omega_B - \omega)^2}{(q_B v_T)^2}\right. \\ &\left. - \frac{q_B^2}{8mT}\right] I_N\left(\frac{q^2 a_B^2}{2 \sinh \alpha}\right). \end{aligned} \quad (7.2)$$

Here  $n$  is the 3D electron concentration,  $v_T = \sqrt{2T/m}$ .

Under the MPR condition  $\mathcal{N}\omega_B = \omega$ , the integral over  $q_B$  diverges logarithmically. The resulting logarithm is the big parameter of the theory. The integral is dominated by all  $q_B$  from  $\sqrt{2mT}$  up to  $\sqrt{2mT}$ . For  $q_B \sim q_T = mv_T/\hbar$  the condition involving Eq. (7.1) can be rewritten as

$$T \lesssim \frac{4\pi e^2 a_B^2}{\varepsilon_{\infty} k_B} \frac{\Gamma_n}{(\omega_l - \omega_t)}. \quad (7.3)$$

For  $a_B \approx 7 \times 10^{-7} \text{ cm}^{-2}$  ( $\mathcal{N}=3$ ) we have  $T \lesssim 10^{-16} n$ ; if one gives here the electron concentration in  $\text{cm}^{-3}$  one gets the temperature in K. Thus to reach a relevant MPR temperature

range, one needs the electron concentrations of the order of  $10^{18} \text{ cm}^{-3}$ . However, such big concentrations are inevitably associated with the electron scattering by the doping impurities. Therefore all the 3D MPR experiments are performed at much lower concentrations. Thus for  $q \sim q_T$  the effect we are discussing is of no importance.

Considering the interval of  $q_B$  of the order of  $\sqrt{2m\Gamma_e}$ , one can use for the characteristic width of  $\Pi^{(3)}$  the estimate  $\sqrt{T\Gamma_e}$ . As a result, one will have on the left-hand side of inequality (7.3)  $\sqrt{T\Gamma_e}$ . The corresponding limitation on the electron concentration is somewhat weaker than above but still rather difficult to satisfy.

This means that for the 3D case the MPR condition is

$$\mathcal{N}\omega_B = \omega_l. \quad (7.4)$$

### VIII. CONCLUSIONS

Almost four decades have elapsed since the theoretical prediction and subsequent experimental observation of MPR in 3D semiconductor structures. Eventually, along with cyclotron resonance, MPR became one of the main instruments of semiconducting compound spectroscopy.

The advances in semiconductor nanofabrication and material science in recent years have made available materials of great purity and crystalline perfection. The essence of electrical conduction in these structures is that the quantum nature of the electron leaves its distinct trace in a macroscopic measurement. The electrical conduction and some other transport phenomena in such nanoscale structures has been a focus of numerous investigations, both theoretical and experimental, with a number of important discoveries and even patent applications. In particular, the discovery of MPR in the quantum wells took place.<sup>5</sup> After this first publication a number of papers appeared where various aspects of this physical phenomenon were investigated. In the present paper we offer a theoretical interpretation of a number of experimental results.

To summarize, in a polar semiconductor, mixed optic-phonon-magnetoplasmon vibrations can be trapped within a quantum well. Such localized vibrations *interact much more effectively* with the confined electrons of the quantum well than the bulk optic phonons. For  $B$  perpendicular to the plane of quantum well and rather big electron concentrations  $n_s$ , such vibrations are responsible for the *magnetophonon resonance* oscillation of the conductivity of quantum wells. As a result, the phonon frequency determining the MPR is shifted towards  $\omega_l$ . The interval of electron concentrations where MPR is observable is estimated and appears to be rather narrow. The estimates qualitatively coincide with the experimental findings.<sup>23</sup> Outside this concentration interval one cannot observe MPR near  $\omega_l/\mathcal{N}$ . To observe MPR at  $\omega_l/\mathcal{N}$  one needs structures with very small effective masses (where big values of  $\omega_B$  can be achieved) and unrealistically big electron damping or exceptionally low values of the electron concentration  $n_s$ . Unlike the 3D case, in the 2D case *the phonon damping often determines the MPR amplitude*.

We also show that the MPR in quantum wells for perpendicular orientation of  $B$  is on practice not as universal as in the 3D case. In particular, its investigation does not permit us to obtain directly the electron's effective mass by measure-

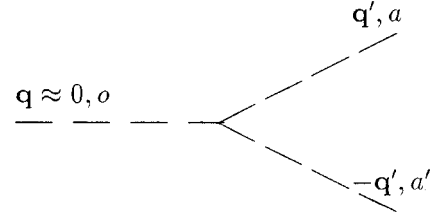


FIG. 6. Decay of an optic phonon into two acoustic ones.

ment of the MPR frequencies. It permits us, however, to investigate various aspects of interaction of electrons belonging to a quantum well with optic phonons as well as other features of behavior of electrons in magnetic field.

### ACKNOWLEDGMENTS

The authors are grateful to M. I. Dyakonov, Y. M. Galperin, and M. L. Shubnikov for a number of interesting discussions. Thanks are due to M. O. Safonchik for his valuable help in performing the numerical calculations. V.V.A. and V.L.G. are grateful to the Wihuri Foundation for a partial support of this work and to Turku University for hospitality. They also acknowledge a partial support for this work by the Russian National Fund of Fundamental Research (Grant No. 97-02-18286-a).

### APPENDIX A: CALCULATION OF $\Gamma$

The damping parameter  $\Gamma$  is determined by the lattice anharmonicity. It is given by the diagram in Fig. 6. Applying the usual rules of the diagrammatic techniques we have

$$\begin{aligned} \Gamma(\omega) = & \frac{\pi\hbar}{8\rho} \sum_{a,a'} \int \frac{d^3q'}{(2\pi)^3} \frac{|b_{oaa'}(0, \mathbf{q}', -\mathbf{q}')|^2}{\omega\omega_a(\mathbf{q}')\omega_{a'}(\mathbf{q}')} \\ & \times \delta[\omega - \omega_a(\mathbf{q}') - \omega_{a'}(-\mathbf{q}')] [N(\omega_a) + 1] \\ & \times [N(\omega_{a'}) + 1]. \end{aligned} \quad (A1)$$

Here the summation is over the three acoustic branches; an extra factor 1/2 is introduced in order not to take into account the same terms twice.

The diagram in Fig. 6 describes the decay of an optic phonon into two acoustic ones belonging to the branches  $a$  and  $a'$ . The corresponding anharmonic interaction is given by the Hamiltonian (cf. Ref. 24)

$$\begin{aligned} \mathcal{H}_{\text{anh}} = & \sum_{\mathbf{q}, \mathbf{q}'} \sum_{a, a'} \frac{(\rho S a)^{1/2} \hbar}{2\rho V} \\ & \times b_{oaa'}(\mathbf{q}, \mathbf{q}', -\mathbf{q}) c_{o\mathbf{q}} c_{a\mathbf{q}'}^\dagger c_{a' - \mathbf{q}'}^\dagger \\ & \times [\omega\omega_a(\mathbf{q}')\omega_{a'}(\mathbf{q}')]^{-1} + \text{H.c.}, \end{aligned} \quad (A2)$$

where  $\rho$  is the mass density,  $S$  is the area of the quantum well,  $b_{oaa'}$  are the so-called anharmonic coefficients (see Ref. 24, Sec. 6),  $c_{o\mathbf{q}}$  is the operator of annihilation of an optic phonon, and  $c_{a, \mathbf{q}}^\dagger$  is the operator of creation of acoustic phonon. Characteristic values of the acoustic phonon frequencies in the integral [Eq. (A1)] are about  $\omega_l/2$ . Then the characteristic values of  $q'$  are of the order of  $\pi/a_o$  where  $a_o$

is the lattice constant. This means that the absolute values  $q$  are much smaller than  $q'$ . This is why in Eq. (A1)  $q$  can be replaced by 0.

According to Ref. 24, Sec. 7 we have the following rough order-of-magnitude estimate for the anharmonic coefficients:

$$|b_{aaa'}(\mathbf{q}, \mathbf{q}', -\mathbf{q}' - \mathbf{q})| \approx \eta_{\mathbf{q}} \frac{s^2}{a_0^3}, \quad (\text{A3})$$

where  $s$  is some average value of the sound velocity while  $\eta_{\mathbf{q}}$  is a  $\mathbf{q}$ -dependent dimensionless numerical factor determined by the anharmonicity. Usually it is somewhat bigger than unity.

For low temperatures

$$k_B T \ll \hbar \omega_l. \quad (\text{A4})$$

Equation (A1) is temperature independent. Taking into account Eq. (A2) we get the following estimate:

$$\Gamma \approx \frac{\eta \hbar \omega_l}{\rho a_0^3 s^2}, \quad (\text{A5})$$

where  $\eta$  is a dimensionless numerical coefficient characterizing the anharmonicity. Its typical value is several units. We do not believe that its theoretical calculations can at present provide sufficient accuracy because of a limited volume of the well and a possible small lattice mismatch. This is why we think that the results of Ref. 25 are not directly applicable in this case and that experimental determination of  $\Gamma$  should be more reliable. In other words,  $\Gamma$  for the phonons trapped near a quantum well can differ substantially from  $\Gamma$  for the bulk optic phonons.

The damping parameter  $\Gamma$  goes up with temperature at such temperatures when the terms with Bose functions in Eq. (A1) begin to play a role (cf. Ref. 25). This is one of the sources of temperature dependence of the amplitude of MPR oscillation.

## APPENDIX B: ROLE OF DISPERSION OF OPTIC VIBRATIONS

We start with the expression for the phonon propagator with regard to the dispersion (neglecting the anisotropy of dispersion). To take the dispersion into account one has to replace in the denominators of Eq. (5.2):

$$\omega_l \rightarrow \sqrt{\omega_l^2 - \beta^2(q^2 + k^2)}, \quad (\text{B1})$$

where  $\beta$  has units of velocity and is equal for GaAs according to Ref. 26  $4.7 \times 10^5 \text{ cm s}^{-1}$ . Then

$$\varepsilon(\omega, \mathbf{q}, k) = \varepsilon_\infty \frac{\omega_l^2 - \beta^2(q^2 + k^2) - \omega^2}{\omega_l^2 - \beta^2(q^2 + k^2) - \omega^2}. \quad (\text{B2})$$

Thus taking into account the nonhomogeneity along the  $z$  direction, one is not allowed to take  $\varepsilon(\omega, \mathbf{q}, k)$  out of the integral over  $k$  in Eq. (4.3). Assuming for simplicity the well's width to be much smaller than  $a_B$ , one gets for the full propagator Eq. (4.3), after integration over  $k$ , the following additional term:

$$- \frac{2\pi\beta e^2}{\varepsilon_\infty} \frac{(\omega_l^2 - \omega^2)}{[(\omega \pm i\Gamma)^2 - \omega_l^2] \sqrt{\omega_l^2 - \omega^2}}. \quad (\text{B3})$$

Here we have assumed that

$$\frac{\Gamma}{\omega_l - \omega_l} \ll 1. \quad (\text{B4})$$

We have omitted here the terms proportional to  $\Gamma\beta$  that would have given an insignificant variation of the width of resonance. One can get the shift of the maximum by replacement

$$\Gamma^2 \rightarrow \Gamma^2 + \sqrt{\omega_l^2 - \omega_l^2} \beta / a_B$$

in Eq. (6.2). Inserting the typical values of the parameters we see that the shift is of the order of 1 K.

<sup>1</sup>Yu. A. Firsov, V. L. Gurevich, R. V. Parfeniev, and I. M. Tsidil'kovskii, in *Landau Level Spectroscopy*, edited by G. Landwehr and E. I. Rashba (Elsevier, Amsterdam, 1991).  
<sup>2</sup>V. L. Gurevich and Yu. A. Firsov, *Zh. Eksp. Teor. Fiz.* **40**, 199 (1961) [*Sov. Phys. JETP* **13**, 137 (1961)].  
<sup>3</sup>S. M. Puri and T. H. Geballe, *Bull. Am. Phys. Soc.* **8**, 309 (1963).  
<sup>4</sup>S. S. Shalyt, R. V. Parfeniev, and V. M. Muzhdaba, *Fiz. Tverd. Tela. (Leningrad)* **6**, 647 (1964) [*Sov. Phys. Solid State* **6**, 508 (1964)].  
<sup>5</sup>D. C. Tsui, Th. Englert, A. Y. Cho, and A. C. Gossard, *Phys. Rev. Lett.* **44**, 341 (1980).  
<sup>6</sup>Th. D. Englert, D. C. Tsui, J. C. Portal, J. Beerens, and A. C. Gossard, *Solid State Commun.* **44**, 1301 (1982).  
<sup>7</sup>G. Kido, N. Miura, H. Ono, and H. Sakaki, *J. Phys. Soc. Jpn.* **51**, 2168 (1982).  
<sup>8</sup>M. A. Brummel, R. J. Nicholas, M. A. Hopkins, J. J. Harris, and C. T. Foxon, *Phys. Rev. Lett.* **58**, 77 (1987).  
<sup>9</sup>R. Kubo, H. Hasegawa, and N. Hashitsume, *J. Phys. Soc. Jpn.* **14**, 56 (1956).  
<sup>10</sup>H. Frölich, *Proc. R. Soc. London, Ser. A* **160**, 230 (1937).

<sup>11</sup>L. D. Landau and E. M. Lifshitz, *Quantum Mechanics, Non-Relativistic Theory* (Pergamon, New York, 1996).  
<sup>12</sup>H. Sato and Y. Hori, *Phys. Rev. B* **39**, 10 192 (1989).  
<sup>13</sup>V. L. Gurevich and K. E. Shtengel, *Phys. Rev. B* **44**, 8825 (1991); *J. Phys.: Condens. Matter* **2**, 6323 (1990).  
<sup>14</sup>E. M. Lifshitz and L. P. Pitaevskii, *Statistical Physics* (Pergamon, New York, 1990), Vol. 2.  
<sup>15</sup>E. H. Sondheimer and A. H. Wilson, *Proc. R. Soc. London, Ser. A* **210**, 173 (1951).  
<sup>16</sup>N. Mori, H. Murata, K. Taniguchi, and C. Hamaguchi, *Phys. Rev. B* **38**, 7622 (1988).  
<sup>17</sup>V. I. Gurevich, A. I. Larkin, and Yu. A. Firsov, *Fiz. Tverd. Tela. (Leningrad)* **4**, 185 (1962) [*Sov. Phys. Solid State* **4**, 131 (1962)].  
<sup>18</sup>O. K. Kim and W. G. Spitzer, *J. Appl. Phys.* **50**, 4362 (1979).  
<sup>19</sup>B. D. Laikhtman and E. L. Altshuler, *Ann. Phys. (N.Y.)* **232**, 322 (1994).  
<sup>20</sup>M. E. Raikh and T. V. Shahbazyan, *Phys. Rev. B* **47**, 1522 (1993).  
<sup>21</sup>T. Ando and Y. Uemura, *J. Phys. Soc. Jpn.* **36**, 959 (1974).  
<sup>22</sup>T. Ando, A. B. Fowler, and F. Stern, *Rev. Mod. Phys.* **54**, 437

- (1982).
- <sup>23</sup>R. J. Nicholas, in *Landau Level Spectroscopy*, edited by G. Landwehr and E. I. Rashba (Elsevier, Amsterdam, 1991).
- <sup>24</sup>V. L. Gurevich, *Transport in Phonon Systems* (Elsevier, Amsterdam, 1986).
- <sup>25</sup>A. R. Bhatt, K. W. Kim, and M. A. Stroscio, *J. Appl. Phys.* **76**, 3905 (1994).
- <sup>26</sup>M. Babiker, *J. Phys. C* **19**, 683 (1986).